Article

Enhanced Magnetic Properties and Thermal Conductivity of FeSiCr Soft Magnetic Composite with Al_2O_3 Insulation Layer Prepared by Sol-Gel Process

Qintian Xie [1], Hongya Yu [2,3,*], Han Yuan [2], Guangze Han [1,3,*], Xi Chen [1,3] and Zhongwu Liu [2]

1   School of Physics and Optoelectronics, South China University of Technology, Guangzhou 510640, China
2   School of Materials Science and Engineering, South China University of Technology, Guangzhou 510640, China
3   Dongguan Mentech Optical & Magnetic Co., Ltd., Dongguan 523330, China
*   Correspondence: yuhongya@scut.edu.cn (H.Y.); phgzhan@scut.edu.cn (G.H.)

Abstract: FeSiCr soft magnetic composites (SMCs) were fabricated by the sol-gel method, and an Al_2O_3/resin composite layer was employed as the insulation coating. By the decomposition of boehmite (AlOOH) gel into Al_2O_3 in the temperature range of 606–707 °C, a uniform Al_2O_3 layer could be formed on the FeSiCr powder surface. The Al_2O_3 insulation coating not only effectively reduced the core loss, increased the resistivity, and improved the quality factor, but it also increased the thermal conductivity of SMCs. The best overall properties with saturation magnetization M_s = 188 emu/g, effective permeability μ_e = 39, resistivity ρ = 8.28 × 10^5 Ω·cm, quality factor Q = 94 at 1 MHz, and core loss = 1173 mW/cm^3 at 200 kHz and 50 mT were obtained when the SMC was prepared with powders coated by 0.5 wt.% Al_2O_3 and resin. The optimized SMC exhibited the lowest core loss with 27% reduction compared to the resin only-insulated sample and 71% reduction compared to the sample without insulation treatment. Importantly, the thermal conductivity of the SMCs is 5.3 W/m·K at room temperature, which is higher than that of the samples prepared by phosphating and SiO_2 coating owing to the presence of a high thermal conductive Al_2O_3 layer. The high thermal conductivity is beneficial to enhancing the high temperature performance, lifetime, and reliability of SMCs. This work is expected to be a valuable reference for the design and fabrication of SMCs to be applied in high-temperature and high-frequency environments.

Keywords: soft magnetic composites; sol-gel; magnetic properties; core loss; thermal conductivity

1. Introduction

As we transition to a more electrified and sustainable world, efficient power conversion requires magnetic passive devices to achieve high power density [1]. Soft magnetic materials play an important role in the field of power electronics, and they have been widely used in transformers, inductors, capacitors, etc. Soft magnetic composites (SMCs) are the newest class of soft magnetic materials, consisting of micron-sized particles pressed after insulation treatment [2]. The unique properties of SMCs include isotropic magnetic and thermal properties, high magnetic permeability, low coercivity, a high Curie temperature, reduced weight and size, and low core loss [3,4]. Hence, SMCs are capturing the attention of a growing number of researchers due to these improved electromagnetic properties [5–10].

FeSiCr alloy powder, as one of the most promising soft magnetic materials, has been employed for the preparation of SMCs [11–15]. The addition of Cr to Fe-Si alloys reduces their magnetic anisotropy and improves their corrosion resistance [16]. Insulation coatings are utilized to form the isolation network between ferrous particles so that the core loss generated by eddy currents can be reduced. The coating technology is one of the key factors for fabricating high-performance FeSiCr SMCs [17]. Both organic and inorganic materials have been used for insulation. Although the organic coatings provide satisfactory adhesion

and flexibility, most of them exhibit poor resistance against high-temperature treatment [18]. Inorganic coatings usually exhibit higher thermal stability compared to organic insulations, such as epoxy and phenolic resins [19]. The latest investigations showed that the organic-inorganic composite insulation layers for FeSiCr exhibit the advantages of good adhesion and high resistivity. Guo et al. [10] improved the permeability and resistivity of FeSiCr powder by coating it with different concentrations of NiZn ferrite. Wang et al. [12] provided a new nano-$CaCO_3$/epoxy nanocomposites insulating layer on FeSiCr and carbonyl iron powder, which effectively reduced high-frequency losses. Xia et al. [17] explored the phosphating process for FeSiCr powders to improve the resistivity of SMCs. However, these studies stopped at the insulation effects, and almost no research related to the thermal conductivity of SMCs has been conducted. In fact, the SMC devices applied in AC fields are accompanied by heat generation. Excessive temperature of the magnetic core will cause a reduction in the performance of the devices or even overheating damage to the core. A high thermal conductivity of SMCs can quickly release the heat produced by magnetic losses and thus enhance the performance, lifetime, and reliability of SMCs and devices [20]. As we all know, Al_2O_3 is a metal oxide with high resistivity and temperature resistance, which is also widely used as a thermal transfer filler in polymer composites owing to its high thermal conductivity [21,22]. The thermal conductivities of typical inorganic coatings at room temperature for iron phosphate, SiO_2, Al_2O_3, and soft ferrites are 0.8–2 W/m·K [23], 0.27 W/m·K, 30 W/m·K [24], and 0.1–0.3 W/m·K [25], respectively. Al_2O_3, as an easily prepared metal oxide with both high thermal conductivity and high resistivity, is thus a good insulation layer material for SMCs. Therefore, it is expected that the magnetic performance and thermal stability of SMCs can be enhanced by an Al_2O_3 inorganic layer.

In this work, an Al_2O_3 insulation layer was successfully prepared on the surface of FeSiCr powders using the sol-gel method. The thickness of the Al_2O_3 insulation layer was controlled by the solid content of boehmite (AlOOH) sol. The microstructure and magnetic properties of the SMCs with insulation layers containing different Al_2O_3 contents were investigated. The results showed that the SMCs insulated by Al_2O_3/resin composites have significantly improved resistivity, frequency stability of permeability, core loss, and thermal conductivity. This work provides a viable solution for the fabrication of high magnetic performance and temperature-resistant SMCs.

2. Experimental Methods

2.1. SMC Preparation

The raw FeSiCr powders with a mean particle size of 10 μm were commercially purchased from Antai Technology Co., Ltd (Beijing, China)., and they had the composition of 88.5–90.5 wt.% Fe, 4.5–5.5 wt.% Si, and 5–6 wt.% Cr. $Al(OPr^i)_3$ (Macklin) was used as the precursor for the hydrolysis reaction to obtain the Al_2O_3. Silicone (KR5235) and epoxy resin (AFG90H) supplied by Shin-Etsu Chemical Co., Ltd (Tokyo, Japan). and Tiantai New Materials Co., Ltd (Guangzhou, China)., respectively, were used as the binder to improve the moldability and strength of the powders. KH550 (Usolf) silane coupling agent was used to improve the binding between the organic and inorganic composite coatings. All chemicals used were of an analytical grade and could be used without further purification in this work.

The $Al(OPr^i)_3$, ground into powder, was added to deionized water and heated to 85 °C with mechanical stirring. After 30 min, nitric acid was added as a precipitating solubilizer and catalyst. Afterward, stable and transparent AlOOH sol was obtained by continuous mechanical stirring at 85 °C for 5 h. The molar ratio of $Al(OPr^i)_3$, deionized water, and nitric acid was 1:90:0.3. AlOOH sols with different solid contents (0.5–2.0 wt.%) were mixed and coated with FeSiCr powders under 105 °C until the solvent was evaporated. The mixed powders were subsequently calcined at 700 °C under a high vacuum pure argon atmosphere for 1 h to obtain the Al_2O_3 layer. Phosphated and SiO_2-coated samples with similar resin bonding were fabricated by the conventional phosphating process [26] and TEOS hydrolysis [5], respectively, to compare the thermal conductivity.

The organic coating solution was prepared by dissolving 1 wt.% epoxy-modified silicone resin and 0.5 wt.% KH550 in acetone. The previously obtained powders were dipped into the organic coating solution and stirred until the acetone evaporated. Subsequently, the composite powders and 0.5 wt.% of the lubricant barium stearate were compacted at 1200 MPa into toroidal-shaped SMCs with the dimensions of $\Phi20 \times \Phi12 \times 4.6$ mm. It should be mentioned that the size of our tested samples was not based on the international standards but on the technique requirements of Mentech Optical & Magnetic Co., Ltd (Dongguan, China). Similar sample dimensions have also been used in some studies of FeSiCr SMCs from other research groups [12,13,15]. Finally, the SMCs were heated to 180 °C for 2 h to cure the resin. A schematic diagram of the preparation process of FeSiCr SMCs is presented in Figure 1.
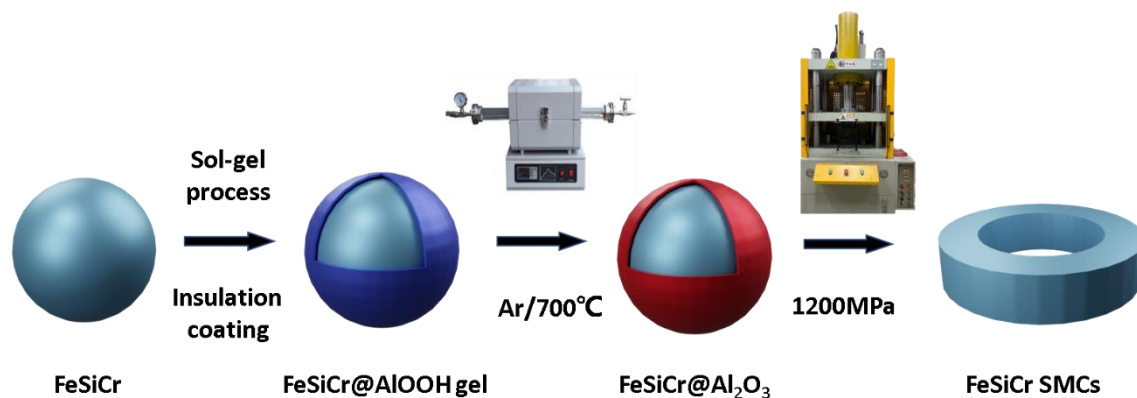

Figure 1. Schematic diagram of the preparation process of FeSiCr SMCs.

2.2. Characterizations

The surface morphologies of the powders and a cross-section of the SMCs were observed by scanning electron microscopy (SEM, FEI Quanta 200, Hillsboro, OR, USA) with energy dispersive X-ray spectroscopy (EDS, EDAX Genesis Xm 2, Pleasanton, USA). Differential thermal analysis (DSC, STA449C, Netzsch, Bavaria, Germany) was used to scan the thermal variation of the FeSiCr coated by AlOOH gel in an argon atmosphere heated to 900 °C at a heating rate of 10 K/min. Fourier transform infrared spectroscopy (FTIR, VERTEX 70, Bruker, Billerica, MA, USA) was used to investigate the chemical structure and state of the coatings at 400–4000 cm^{-1} transmittance. The phase structures of powders before and after insulation treatment were confirmed by X-ray diffraction (XRD, Philips X' Pert, PANalytical, Almelo, The Netherlands) using Cu Kα radiation at room temperature. The electrical resistivity was measured by a high resistance weak current tester (ST2643, Jingge, Suzhou, China). The density was calculated based on the weight and size of the SMC core. The hysteresis loops were measured at room temperature using a Vibrating Sample Magnetometer (VSM-3105, East Changing, Beijing, China). An impedance analyzer (Agilent E4990A, Keysight, Beijing, China) was used to measure the permeability μ_e and quality factor Q of SMCs from 20 kHz to 10 MHz, with contact electrodes in a double-ended configuration. μ_e can be defined as follows:
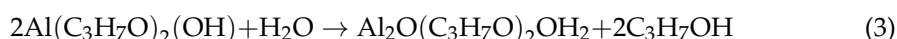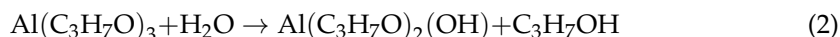
$$\mu_e = \frac{L}{2h \times \ln(D/d) \times N^2 \times 10^{-10}} \tag{1}$$

where L is the effective self-inductance, N is the number of copper wire turns, h is the height of the sample, and D and d are the outer and inner diameters of the sample, respectively. The core losses were measured using a soft magnetic AC test set (MATS-3010SA, Linkjoin, Loudi, China) at B_m = 50 mT, 20–200 kHz. The thermal conductivity of strip block-pressed SMCs was measured using a physical property measurement system (PPMS-9).
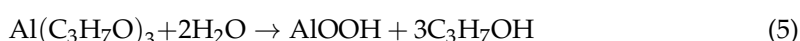
3. Results and Discussion

3.1. Structure Analysis

By the hydrolysis of $Al(OPr^i)_3$, the Al_2O_3 insulating layer was coated on the FeSiCr powders [27]. The main hydrolysis process can be described with the following three equations:

$$Al(C_3H_7O)_3 + H_2O \rightarrow Al(C_3H_7O)_2(OH) + C_3H_7OH \tag{2}$$

$$2Al(C_3H_7O)_2(OH) + H_2O \rightarrow Al_2O(C_3H_7O)_2OH_2 + 2C_3H_7OH \tag{3}$$

$$Al_2O(C_3H_7O)_2OH_2 + H_2O \rightarrow 2AlOOH + 2C_3H_7OH \tag{4}$$

The total reaction is:

$$Al(C_3H_7O)_3 + 2H_2O \rightarrow AlOOH + 3C_3H_7OH \tag{5}$$

Since the whole hydrolysis reaction is conducted in solution, the resulting product of boehmite (AlOOH) particles is easily and uniformly dispersed in the solution at the molecular level. During preparation, these particles cover the powders as an insulating layer, which will be pyrolyzed into Al_2O_3 by subsequent annealing. The by-product of propyl alcohol has a low boiling point and thus mostly evaporates during the heating.

During the sol-gel process, the solute is aged, and the colloidal pellets slowly polymerize to form a gel with a three-dimensional spatial network structure. After drying, sintering, and curing the gel, a molecular and even nanostructured coating layer could be formed on the powders. To explore the dehydration temperature of the AlOOH gel, the DSC curve of the FeSiCr powders coated by AlOOH gel was tested, as shown in Figure 2. Although the insulation layer is thin, there is still an obvious heat absorption peak with an area of $\Delta H = 1.47$ J/g of heat absorption per unit, which is obtained by calculating the peak area on the baseline based on the integration. The decomposition of boehmite gel begins at 660 °C, and this reaction is practically complete by 707 °C. This reaction can be described by the following equation [28]:

$$2\alpha - AlOOH \rightarrow \gamma - Al_2O_3 + H_2O \tag{6}$$
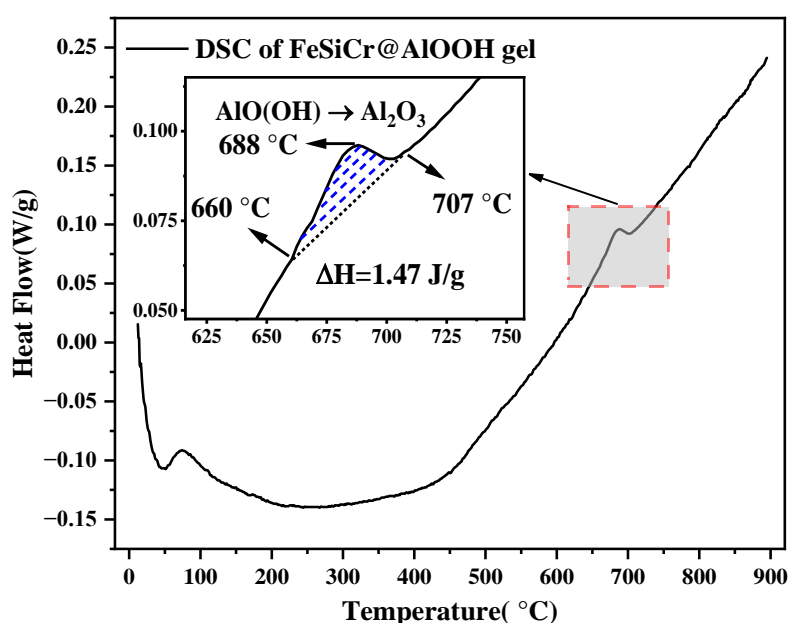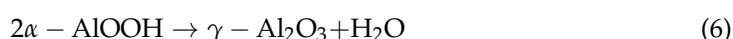

Figure 2. The DSC curve of the FeSiCr powder coated by AlOOH gel.

A lower annealing temperature is needed not only for the consideration of energy savings but also to minimize partial oxidation, which may deteriorate the magnetic permeability. The peak point of the DSC curve corresponds to the fastest energy change, which is 688 °C, as shown in Figure 2. In this work, a temperature of 700 °C, slightly higher than 688 °C, was chosen as the heating temperature to obtain more physically stable Al_2O_3 coating.

FTIR analysis was performed on the FeSiCr powders coated by AlOOH gel before and after heating at 700 °C to understand the evolution of the insulating coatings during the heating process, as shown in Figure 3. The FTIR spectrum, taken from the uncoated powders, is also shown in Figure 3 for comparison. The broad absorption bands around 3430 cm^{-1} and 1630 cm^{-1} are attributed to the stretching of -OH [29], while the weakening of the -OH vibration of the coated powders is due to the formation of Al-O-Al metal bonds by dehydration of the solute with the surface -OH sites. The absorption bands at 490 cm^{-1} and 435 cm^{-1} are attributed to the Si-O and Fe-O vibrations due to trace oxidation appearing on all sample surfaces [5,30]. Compared to uncoated powder, the new 1060 cm^{-1} and 1160 cm^{-1} absorption bands correspond to the Al-OH vibration of the boehmite AlOOH [19,31], and the absorption band around 609 cm^{-1} corresponds to Al-O-Al [32,33]. It indicates that an insulating layer of AlOOH gel and Al_2O_3 has been formed on the powder surface [31,33]. Due to the high-temperature pyrolysis that converts the AlOOH gel into alumina, the sample after heating at 700 °C for 1 h showed a significantly enhanced Al-O-Al vibration at 609 cm^{-1} compared to the untreated sample. At the same time, the bands around 1380 cm^{-1} and 887 cm^{-1} originating from Fe-OH and Fe-O were observed due to a small amount of oxidation of the powder after heating [34].
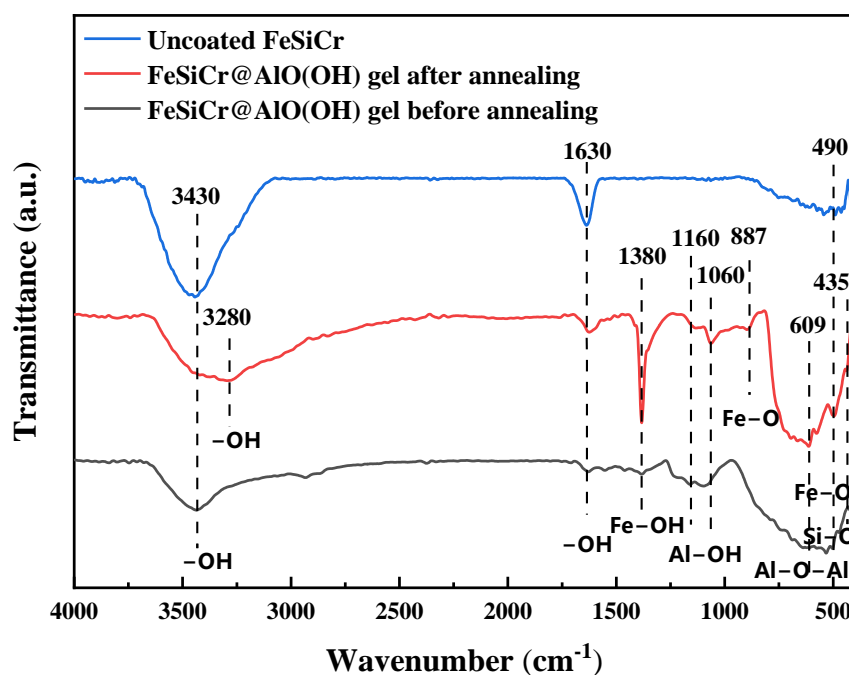

Figure 3. FTIR spectra of the raw FeSiCr powders and the powders insulated by AlOOH gel before and after annealing at 700 °C for 1 h.

The phase structures of powders before and after insulation treatment are shown in Figure 4. The uncoated FeSiCr powder and all Al_2O_3 coated composite powders exhibited sharp crystallization peaks at 44.8°, 65.2°, and 82.6° with crystallographic indices of (110), (200), and (211), respectively, which are typical of the characteristic peaks of α-Fe(Si,Cr). The obvious Al_2O_3 diffraction peaks were not clearly detected. The reasons can be attributed to the content of the formed Al_2O_3 being very low or the heating temperature not reaching

the crystallization temperature of Al_2O_3. Nevertheless, this outcome does not disprove that there is an alumina insulation layer generated on the powder surface.
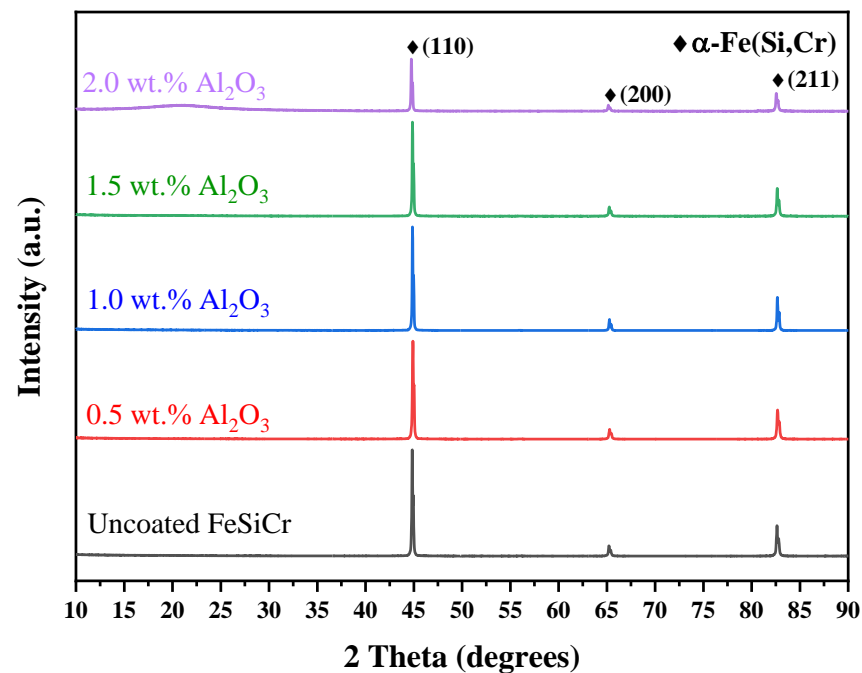

Figure 4. X-ray diffraction (XRD) of uncoated and different Al_2O_3-coated FeSiCr powders.

Figure 5 shows the morphologies and EDS elemental distribution of the FeSiCr powders insulated by different concentrations of the Al_2O_3 layer. The 0.5 wt.% Al_2O_3-coated powder showed a slight, rough surface, and no significant change could be observed compared to the raw powders in Figure 5a because the thickness of the layer is very thin. In Figure 5b, the detected Fe, Si, and Cr elements came from the initial powder. The Al and O elements exhibited the same uniform distribution. The mass ratio of the Al element increased with the gradual increase in the solid content of Al_2O_3 in the boehmite sols. At the same time, a thicker surface insulation layer is clearly revealed in Figure 5c,d. The 1.5 wt.% Al_2O_3-coated powder became rough, and a few visible flocs gathering appeared on the powder surface, as shown in Figure 5d. The mass ratio of the Al element is significantly increased compared to the low concentration of the Al_2O_3-coated powder. According to the SEM results, there is a thin Al_2O_3 insulation layer covering the powder, and the thickness was affected by the Al_2O_3 concentration. To provide maximum permeability and density, the amount of interparticle insulation should be minimized. A thin and uniform insulation layer is generally required to minimize the eddy current in high-frequency applications.

The polished cross-section of the SMCs is shown in Figure 6. The EDS result of line scanning crossing the powder interface indicates that the Al and O elements appear at the interface of particles containing Fe elements. The elemental distribution on particle boundaries indicates that the particles are isolated by the alumina insulating layer. The coating layer forms the isolation network between ferrous particles, which can reduce the powder contact and even act as a heat conduction channel. In addition, air gaps can still be found between the particles under pressure of 1200 MPa. Partial extrusion deformation can also be observed. Partial deformation can reduce the porosity and increase the density, but this additional deformation induces high stress and thus may increase the hysteresis loss [35]. The internal stress introduced during compaction can often be relaxed in the post-annealing process.
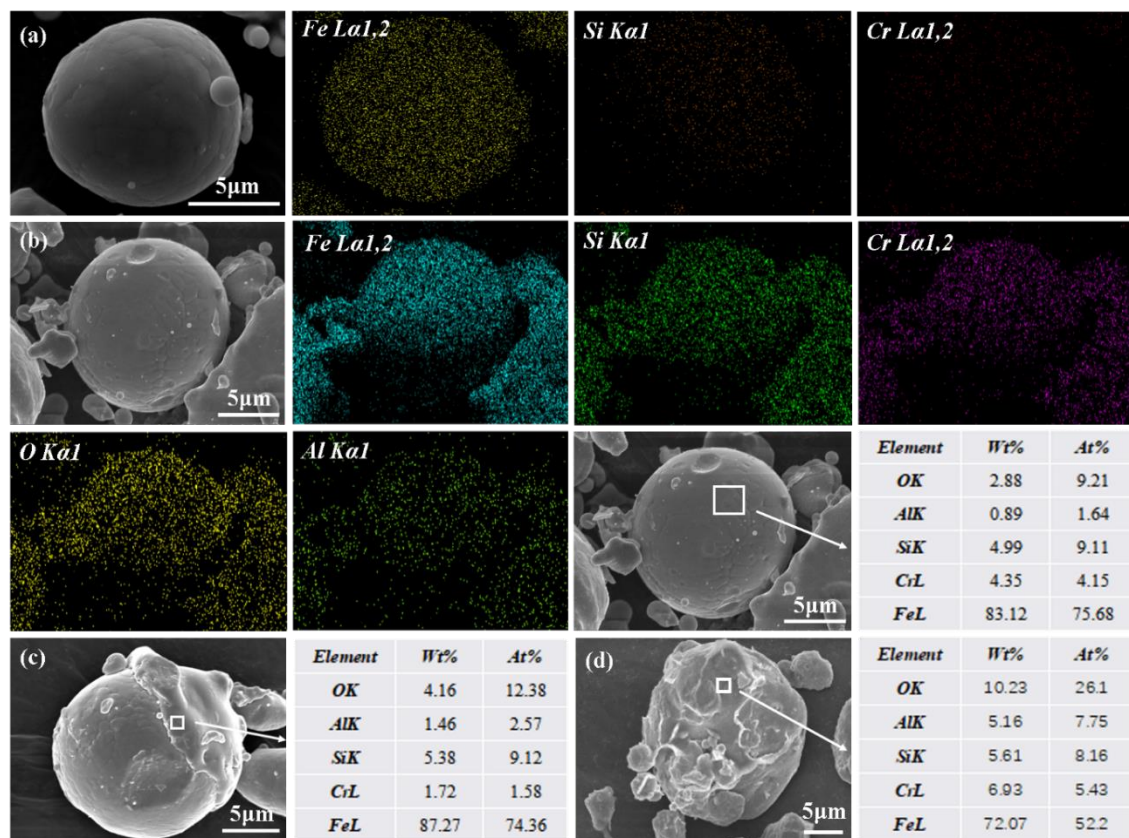
Figure 5. SEM micrograph and EDS elemental distribution maps of the FeSiCr powders insulated by different Al_2O_3 concentrations: (**a**) raw powder; (**b**) 0.5%; (**c**) 1.0%; and (**d**) 1.5%.
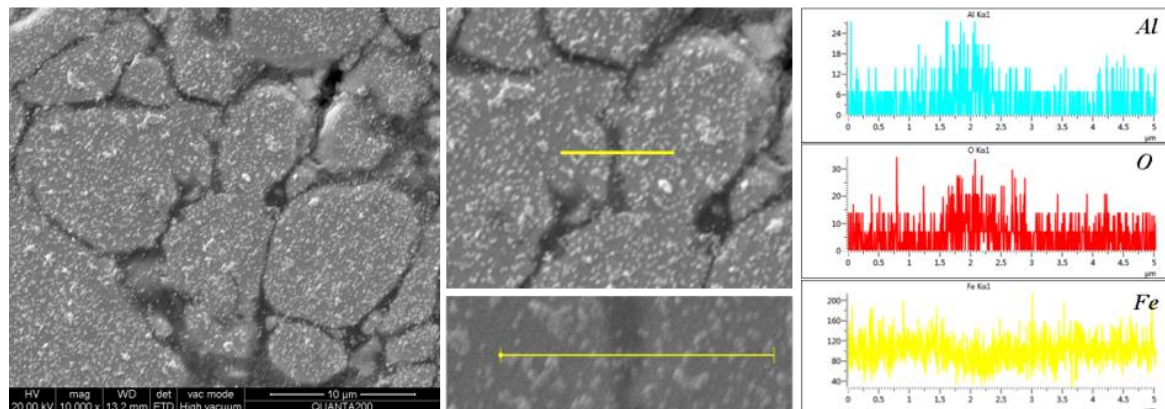

Figure 6. SEM micrograph and EDS analysis (line scanning) of the cross-section of FeSiCr@Al_2O_3 SMCs.

3.2. Magnetic Performance

Figure 7 illustrates the magnetic hysteresis loops of FeSiCr powders coated with different Al_2O_3 contents. The enlarged image shows the saturation magnetization M_s. Compared to the uncoated powders, as the content of Al_2O_3 increases to 2.0 wt.%, the M_s value decreases monotonically from 193 emu/g to 177 emu/g due to the magnetic dilution effect of the non-magnetic substance Al_2O_3. This result indicates that the introduction of inorganic insulation coating does not significantly reduce the M_s of the magnetic powder, and M_s remains in the normal level of FeSiCr powder (130–200 emu/g) [12]. Combined with the content and morphology of the insulating layer within Figure 5, the introduced Al_2O_3 insulating layer is thin, with less influence on the deterioration of the original powder M_s.
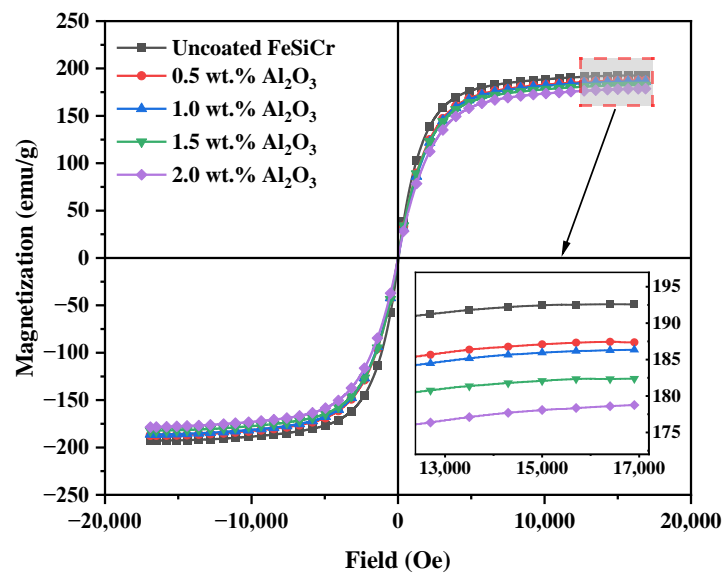
Figure 7. The magnetic hysteresis loops for different Al_2O_3-coated FeSiCr powders.

The effective permeability μ_e variation with the frequency for different contents of Al_2O_3 coatings are shown in Figure 8. The samples fabricated by raw powders exhibit poor frequency stability of μ_e, and as the frequency increases to 5 MHz, the μ_e decrease monotonically drops from 55 to 21 (a decrease of 62%) subjected to the deteriorating effect of eddy currents. All the Al_2O_3/resin-coated SMCs have almost constant permeability from 20 kHz to 5 MHz, due to the good insulation between the magnetic powders. After a 1 wt.% resin coating, the μ_e decreases from 55 to 40 (a decrease of 28%), while a further reduction from 40 to 34 (a decrease of 15%) appears with the increasing concentration (0–2 wt.%) of Al_2O_3. This decrease is due to the magnetic dilution effect of Al_2O_3 and resin, as well as the introduction of more air gaps and cracks into the insulation layer. It can be concluded from the reduction percentage of μ_e that the addition of resin has a greater effect on the decrease in magnetic permeability than the Al_2O_3 layer. Thus, the 0.5 wt.% Al_2O_3/resin coating sample causes a minor decrease in μ_e compared to the resin-only coating sample, whereas the μ_e decreased only from 40 to 39.
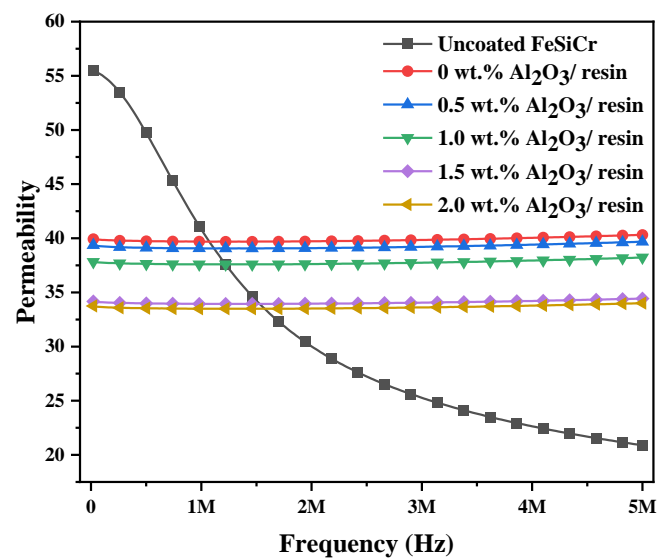

Figure 8. Permeability of FeSiCr SMCs with different contents of Al_2O_3 insulation versus frequency (from 20 kHz to 5 MHz).

The core loss is the dissipating part of energy that is converted irreversibly into heat through the periodically magnetized process. In the current application frequency field, the total loss mainly consists of hysteresis loss, eddy current loss, and anomalous loss. Hysteresis loss is due to the irreversible domain wall displacement and magnetization vector rotation. The AC magnetic process generates eddy currents, which depend on the inductive magnetic field and frequency in working conditions. Anomalous loss is a combination of relaxation and resonant losses. According to the classical loss theory, the total loss (W_t) is mainly determined by hysteresis loss (W_h), eddy current loss (W_e), and anomalous loss (W_a) according to the following formula [36,37]:

$$W_t = W_h + W_e + W_a \approx \oint H \mathrm{d}B + \frac{C_e B^2 d^2}{\rho} f + C_a f^{1/2} \tag{7}$$

where f is the frequency, H is the magnetic field strength, B is the magnetic induction, C_e and C_a are the proportionality constants, ρ is the resistivity, and d is the thickness of the material. Figure 9 shows the variation of core loss versus frequencies from 20 to 200 kHz at B_m = 50 mT for FeSiCr SMCs with 0–2 wt.% Al_2O_3/resin coatings. The anomalous loss calculated by fitting the experimental results is very small and neglected, which is only important at very low induction levels and very high frequencies [2]. The raw powder pressed sample exhibits the highest total loss, which severely worsens to 4050 kW/m^3 with the increase in frequency to 200 kHz. The presence of a large, nonlinear eddy current loss fraction indicates a large heat generation effect of inter-particle eddy currents without insulation treatment. Compared to the 1 wt.% resin only-coated SMC sample, the SMCs with (0.5–2 wt.%) Al_2O_3/resin showed a significant reduction in core loss. The minimum value of 1173 mW/cm^3 corresponds to the sample with 0.5 wt.% Al_2O_3/resin, which exhibited a 27% reduction compared to the resin only-coated sample and a 71% reduction compared to an uncoated powder sample. This reduction in loss is due to the suppression of eddy currents by the insulation layer. With the increase in Al_2O_3 concentration, the core loss grows gradually because of the increase in hysteresis loss in part. In a ferromagnetic pressing material, Al_2O_3 impurities between the particles and stressed regions give rise to pinning sites that can hinder domain wall motion [38,39], increasing the coercive force and directly increasing the hysteresis loss.
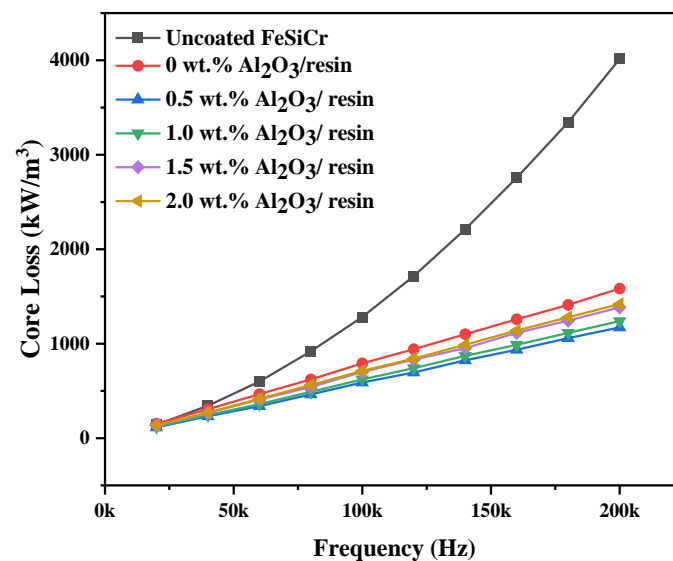

Figure 9. Core losses of FeSiCr SMCs with different contents of Al_2O_3 insulation in the frequency range from 20 kHz to 200 kHz.

Table 1 lists the density, electric resistivity ρ, effective permeability μ_e, and core losses of FeSiCr SMCs insulated with different contents of Al_2O_3. The standard deviations are

calculated by five samples from the same group. The density of SMCs monotonically decreases from 6.31 g/cm^3 of the raw powder to 5.97 g/cm^3 with 2 wt.% Al$_2$O$_3$/resin. The reduction is due to the relatively lower-density insulation layer. The resistivity of the samples after resin-only and 2 wt.% Al$_2$O$_3$/resin coatings increases by nearly 4700 and 1,300,000 times, respectively, compared with the uncoated sample, indicating an increasing trend with the Al$_2$O$_3$ addition. The increasing resistivity can reduce the eddy current between the particles, decreasing the heat dissipation and ensuring the soft magnetic performance of SMCs at high frequencies. In fact, for a test frequency not higher than 200 kHz, an appropriately increased resistivity is able to limit the eddy current loss to a low value, but excessive insulation may increase the hysteresis loss and the total losses. Specifically, as the insulation layer content increases, some properties are optimized with sacrifice of other properties. As shown in Table 1, the resistivity and core losses can be improved, but the permeability and saturation magnetization show some reduction as the Al$_2$O$_3$ content increases. The sample with 0.5% Al$_2$O$_3$-resin showed relatively good properties.

Table 1. The density, resistivity ρ, effective permeability μ_e, and core losses of FeSiCr SMCs insulated with different contents of Al$_2$O$_3$.

Sample (Powder Treatment)	Density (g/cm^3)	Resistivity ρ ($\Omega\cdot$cm)	Permeability (μ_e/200 kHz)	Ps@50 mT/mW/cm^3	
				100 kHz	200 kHz
Uncoated FeSiCr	6.31 ± 0.03	58 ± 9	55.5 ± 1.6	1283 ± 8	4015 ± 26
0% Al$_2$O$_3$-resin	6.23 ± 0.03	(2.8 ± 0.1) × 10^5	39.9 ± 1.2	783 ± 3	1584 ± 11
0.5% Al$_2$O$_3$-resin	6.19 ± 0.02	(8.3 ± 0.5) × 10^5	39.3 ± 1.3	589 ± 3	1173 ± 8
1.0% Al$_2$O$_3$-resin	6.10 ± 0.02	(2.1 ± 0.2) × 10^6	37.8 ± 1.1	620 ± 5	1239 ± 10
1.5% Al$_2$O$_3$-resin	5.98 ± 0.02	(1.9 ± 0.1) × 10^7	34.2 ± 0.9	701 ± 2	1385 ± 5
2.0% Al$_2$O$_3$-resin	5.97 ± 0.02	(7.8 ± 0.2) × 10^7	33.7 ± 0.9	712 ± 5	1420 ± 9

With the demand for high energy storage and low energy dissipation at high frequencies in industrialization, the conversion efficiency is an important characteristic of SMCs. Quality factor *Q* is a vital parameter for the electric component in the circuit. It represents the ratio of energy storage to energy dissipation in inductor devices: a higher quality factor implies better high-frequency soft magnetic performance, which can be understood as follows [40]:

$$Q = \frac{\mu'}{\mu''} \tag{8}$$

where μ' and μ'' are the real and imaginary parts of complex permeability, respectively. Figure 10 shows that the uncoated powder reaches the peak *Q* = 10.3 point at a low frequency (80 kHz) and continuously decreases as the frequency increases. The sample without insulation treatment is only suitable for power conversion at lower frequencies with a lower efficiency. In contrast, the *Q* value of the composite insulated SMCs maintains a high level up to 2~3 MHz, indicating good performance for high-frequency applications. The variation of the *Q* value with Al$_2$O$_3$ content shows the same trend as the core loss (Figure 9), indicating the important, positive effect of insulation treatment for SMCs. The highest quality factor of 94 at 1 MHz also indicates that the 0.5 wt.% Al$_2$O$_3$/resin coating has the best insulation effect.

3.3. Thermal Conductivity

Soft magnetic devices are increasingly required to be used under high electrical current. The thermal stresses due to joule heating and magnetic losses can be damaging. A higher thermal conductivity might improve the thermal performance of the device by increasing the ability to dissipate heat. From the Maxwell–Eucken mixture equation,

an effective thermal conductivity of the composite core material was determined by the following parameters [41]:

$$k_e = k_1 \cdot \left[\frac{k_p + 2 \cdot k_1 + 2 \cdot V_f \cdot (k_p - k_1)}{k_p + 2 \cdot k_1 - V_f \cdot (k_p - k_1)} \right] \tag{9}$$

where k_p and k_1 represent the thermal conductivity of the iron powder and layer, whereas k_e and V_f represent the effective thermal conductivity and volume fraction of the filling, respectively. It can be concluded that k_e is mainly dependent on the layer material. The choice of a higher thermal conductivity coating layer can effectively improve its k_e.
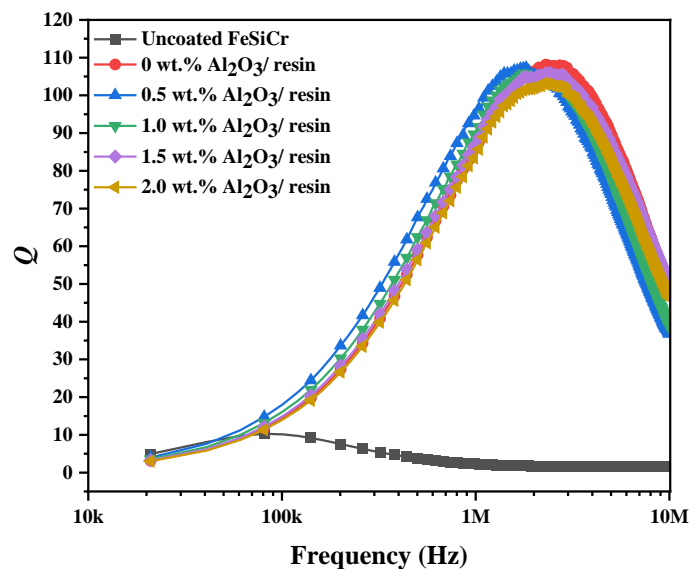

Figure 10. Quality factor Q of FeSiCr SMCs with different contents of Al_2O_3 insulation at the frequency range of 20 kHz to 10 MHz.

The thermal conductivities of FeSiCr-based SMCs with different inorganic layers and similar resin bindings are shown in Figure 11, and they were tested at near room temperature. The thermal conductivity showed a slow decrease with increasing temperature. The conduction of heat within a metal material is mainly achieved by collisions between free electrons. When the temperature increases, the speed of the thermal motion of electrons accelerates, and collisions with lattice dots are more frequent. As a result, the average free range is shortened, and the thermal conductivity decreases. The Al_2O_3-coated sample maintained a higher thermal conductivity, which was ~5.3 W/m·K at room temperature. Using the Maxwell mixture relationship to estimate the thermal conductivity of composites layer k_1, the two parameters were fixed at: $V_f = 0.637$, the maximum fraction to which a volume can be filled with randomly packed spheres; and $k_p = 74$ W/m·K, the thermal conductivity of FeSiCr powders. The calculated thermal conductivity of the Al_2O_3/resin composites layer k_1 is 0.92 W/m·K, which is much higher than the thermal conductivity of general resins (0.11–0.53 W/m·K) [25]. As for the two types of inorganic insulation most commonly used in industrial manufacturing, the phosphating process exhibited higher thermal conductivity than the SiO_2 coating method. This finding is consistent with the trends of the thermal conductivity of these two inorganic insulations themselves. Al_2O_3 insulation layer exhibits the best thermal conducting for the SMCs. It is believed that, as an easily prepared metal oxide with high thermal conductivity, Al_2O_3 insulation treatment will have promising applications for SMC inductor production.
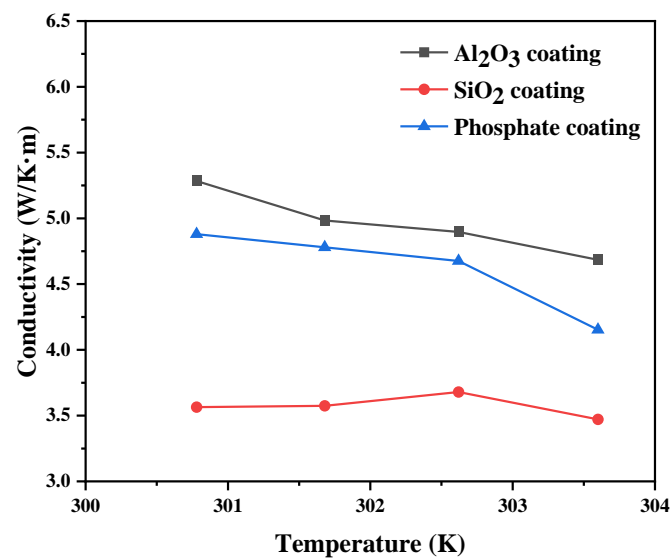
Figure 11. The thermal conductivity of FeSiCr SMCs with different inorganic layers and similar resin bonding values at various temperatures near room temperature.

4. Conclusions

FeSiCr soft magnetic composites (SMCs) based on powder coated with an Al_2O_3/resin insulation layer by the sol-gel method were fabricated. Al_2O_3/resin insulation treatment not only effectively optimized the core loss, resistivity, and quality factor Q of SMCs, but it also improved their thermal conductivity. The sample with 0.5 wt.% Al_2O_3/resin exhibited the optimum comprehensive properties with saturation magnetization M_s = 188 emu/g, effective permeability μ_e = 39, resistivity ρ = 8.28 $\times$ 10^5 Ω·cm, quality factor Q = 94 (at 1 MHz), and core losses = 1173 kW/m^3 (at 200 kHz, 50 mT). The thermal conductivity of SMCs is ~5.3 W/m·K at room temperature, which is higher than that of conventional inorganic coating layers, such as phosphate and SiO_2. The use of inorganic insulating layer techniques allows for stability of μ_e and loss reduction at high frequencies, but it inevitably leads to reductions in μ_e and M_s. The low core loss and high stability of μ_e and high thermal conductivity of SMCs constitute considerable improvements for SMC-based devices to be used in high-frequency and high-temperature environments. This work provides a new strategy for developing SMCs that can work at relatively high temperatures with high reliability, which could be beneficial to high frequencies, miniaturization, and integration of electronic components.

Author Contributions: Formal analysis, Q.X. and H.Y. (Hongya Yu); investigation, X.C.; methodology, Q.X., H.Y. (Han Yuan), G.H. and Z.L.; project administration, H.Y. (Hongya Yu) and Z.L.; supervision, H.Y. (Hongya Yu); visualization, Q.X.; writing—original draft, Q.X.; writing—review and editing, Q.X., H.Y. (Hongya Yu), G.H. and Z.L. All authors have read and agreed to the published version of the manuscript.

Institutional Review Board Statement: Not applicable.

Informed Consent Statement: Not applicable.

Data Availability Statement: Not applicable.

Conflicts of Interest: The authors declare no conflict of interest.

References

1. Silveyra, J.M.; Ferrara, E.; Huber, D.L.; Monson, T.C. Soft magnetic materials for a sustainable and electrified world. *Science* **2018**, *362*, eaao0195. [CrossRef] [PubMed]
2. Shokrollahi, H.; Janghorban, K. Soft magnetic composite materials (SMCs). *J. Mater. Process. Technol.* **2007**, *189*, 1–12. [CrossRef]
3. Sunday, K.J.; Taheri, M.L. Soft magnetic composites: Recent advancements in the technology. *Met. Powder Rep.* **2017**, *72*, 425–429. [CrossRef]
4. Périgo, E.A.; Weidenfeller, B.; Kollár, P.; Füzer, J. Past, present, and future of soft magnetic composites. *Appl. Phys. Rev.* **2018**, *5*, 31301. [CrossRef]
5. Guan, W.W.; Shi, X.Y.; Xu, T.T.; Wan, K.; Zhang, B.W.; Liu, W.; Su, H.L.; Zou, Z.Q.; Du, Y.W. Synthesis of well-insulated Fe–Si–Al soft magnetic composites via a silane-assisted organic/inorganic composite coating route. *J. Phys. Chem. Solids* **2021**, *150*, 109841. [CrossRef]
6. Li, W.; Cai, H.; Kang, Y.; Ying, Y.; Yu, J.; Zheng, J.; Qiao, L.; Jiang, Y.; Che, S. High permeability and low loss bioinspired soft magnetic composites with nacre-like structure for high frequency applications. *Acta Mater.* **2019**, *167*, 267–274. [CrossRef]
7. Li, W.; Li, W.; Ying, Y.; Yu, J.; Zheng, J.; Qiao, L.; Li, J.; Zhang, L.; Fan, L.; Wakiya, N.; et al. Magnetic and Mechanical Properties of Iron-Based Soft Magnetic Composites Coated with Silane Synergized by Bi$_2$O$_3$. *J. Electron. Mater.* **2021**, *50*, 2425–2435. [CrossRef]
8. Yao, Z.; Peng, Y.; Xia, C.; Yi, X.; Mao, S.; Zhang, M. The effect of calcination temperature on microstructure and properties of FeNiMo@Al$_2$O$_3$ soft magnetic composites prepared by sol-gel method. *J. Alloy. Compd.* **2020**, *827*, 154345. [CrossRef]
9. Li, J.; Ni, J.; Zhu, S.; Feng, S. Evolution of magnetic loss with annealing temperature in FeSiAl/carbonyl iron soft magnetic composite. *Mater. Technol.* **2022**, *37*, 2313–2317. [CrossRef]
10. Guo, R.; Wang, S.; Yu, Z.; Sun, K.; Jiang, X.; Wu, G.; Wu, C.; Lan, Z. FeSiCr@NiZn SMCs with ultra-low core losses, high resistivity for high frequency applications. *J. Alloy. Compd.* **2020**, *830*, 154736. [CrossRef]
11. Nie, W.; Yu, T.; Wang, Z.; Wei, X. High-performance core-shell-type FeSiCr@MnZn soft magnetic composites for high-frequency applications. *J. Alloy. Compd.* **2021**, *864*, 158215. [CrossRef]
12. Wang, F.; Dong, Y.; Chang, L.; Pan, Y.; Chi, Q.; Gong, M.; Li, J.; He, A.; Wang, X. High performance of Fe-based soft magnetic composites coated with novel nano-CaCO$_3$/epoxy nanocomposites insulating layer. *J. Solid State Chem.* **2021**, *304*, 122634. [CrossRef]
13. Dong, B.; Qin, W.; Su, Y.; Wang, X. Magnetic properties of FeSiCr@MgO soft magnetic composites prepared by magnesium acetate pyrolysis for high-frequency applications. *J. Magn. Magn. Mater.* **2021**, *539*, 168350. [CrossRef]
14. Hsiang, H.-I.; Chuang, K.-H.; Lee, W.-H. FeSiCr Alloy Powder to Carbonyl Iron Powder Mixing Ratio Effects on the Magnetic Properties of the Iron-Based Alloy Powder Cores Prepared Using Screen Printing. *Materials* **2021**, *14*, 1034. [CrossRef]
15. Gong, M.; Dong, Y.; Huang, J.; Chang, L.; Pan, Y.; Wang, F.; He, A.; Li, J.; Liu, X.; Wang, X. The enhanced magnetic properties of FeSiCr powder cores composited with carbonyl iron powder. *J. Mater. Sci. Mater. Electron.* **2021**, *32*, 8829–8836. [CrossRef]
16. Yu, H.; Zhou, S.; Zhang, G.; Dong, B.; Meng, L.; Li, Z.; Dong, Y.; Cao, X. The phosphating effect on the properties of FeSiCr alloy powder. *J. Magn. Magn. Mater.* **2022**, *552*, 168741. [CrossRef]
17. Xia, C.; Peng, Y.; Yi, Y.; Deng, H.; Zhu, Y.; Hu, G. The magnetic properties and microstructure of phosphated amorphous FeSiCr/silane soft magnetic composite. *J. Magn. Magn. Mater.* **2019**, *474*, 424–433. [CrossRef]
18. Yaghtin, M.; Taghvaei, A.H.; Hashemi, B.; Janghorban, K. Structural and magnetic properties of Fe-Al2O3 soft magnetic composites prepared by sol-gel method. *Int. J. Mater. Res.* **2013**, *105*, 474–479. [CrossRef]
19. Liu, D.; Wu, C.; Yan, M.; Wang, J. Correlating the microstructure, growth mechanism and magnetic properties of FeSiAl soft magnetic composites fabricated via HNO$_3$ oxidation. *Acta Mater.* **2018**, *146*, 294–303. [CrossRef]
20. Monier-Vinard, E.; Bissuel, V.; Laraqi, N.; Daniel, O.; Signing, D. Experimental characterization of DELPHI Compact Thermal Model for Surface-Mounted Soft Magnetic Composite Inductor. In Proceedings of the 2015 21st International Workshop on Thermal Investigations of ICs and Systems (THERMINIC), Paris, France, 30 September–2 October 2015.
21. Ouyang, Y.; Hou, G.; Bai, L.; Li, B.; Yuan, F. Constructing continuous networks by branched alumina for enhanced thermal conductivity of polymer composites. *Compos. Sci. Technol.* **2018**, *165*, 307–313. [CrossRef]
22. Yu, L.; Lirui, S.; Qingyu, W.; Haitao, Q.; Chuncheng, H.; Qingquan, L. Effect of branched alumina on thermal conductivity of epoxy resin. *J. Ind. Eng. Chem.* **2022**, *120*, 209–215.
23. Pinheiro, A.; da Costa, Z.; Bell, M.; Anjos, V.; Dantas, N.; Reis, S. Thermal characterization of iron phosphate glasses for nuclear waste disposal. *Opt. Mater.* **2011**, *33*, 1975–1979. [CrossRef]
24. Chen, H.; Ginzburg, V.V.; Yang, J.; Yang, Y.; Liu, W.; Huang, Y.; Du, L.; Chen, B. Thermal conductivity of polymer-based composites: Fundamentals and applications. *Prog. Polym. Sci.* **2016**, *59*, 41–85. [CrossRef]
25. Joshi, G.; Saxena, N.; Mangal, R. Temperature dependence of effective thermal conductivity and effective thermal diffusivity of Ni-Zn ferrites. *Acta Mater.* **2003**, *51*, 2569–2576. [CrossRef]
26. Li, K.; Cheng, D.; Yu, H.; Liu, Z. Process optimization and magnetic properties of soft magnetic composite cores based on phosphated and mixed resin coated Fe powders. *J. Magn. Magn. Mater.* **2020**, *501*, 166455. [CrossRef]
27. Hu, B.; Jia, E.; Du, B.; Yin, Y. A new sol-gel route to prepare dense Al$_2$O$_3$ thin films. *Ceram. Int.* **2016**, *42*, 16867–16871. [CrossRef]
28. Paulik, F.; Paulik, J.; Naumann, R.; Köhnke, K.; Petzold, D. Mechanism and kinetics of the dehydration of hydrargillites. Part I. *Thermochim. Acta* **1983**, *64*, 1–14. [CrossRef]

29. Padmaja, P.; Anilkumar, G.; Mukundan, P.; Aruldhas, G.; Warrier, K. Characterisation of stoichiometric sol–gel mullite by fourier transform infrared spectroscopy. *Int. J. Inorg. Mater.* **2001**, *3*, 693–698. [CrossRef]

30. Pu, H.; Jiang, F.; Yang, Z. Studies on preparation and chemical stability of reduced iron particles encapsulated with polysiloxane nano-films. *Mater. Lett.* **2006**, *60*, 94–97. [CrossRef]

31. Shen, S.-C.; Ng, W.K.; Zhong, Z.-Y.; Dong, Y.-C.; Chia, L.; Tan, R.B.H. Solid-Based Hydrothermal Synthesis and Characterization of Alumina Nanofibers with Controllable Aspect Ratios. *J. Am. Ceram. Soc.* **2009**, *92*, 1311–1316. [CrossRef]

32. Peng, Y.; Yi, Y.; Li, L.; Yi, J.; Nie, J.; Bao, C. Iron-based soft magnetic composites with Al_2O_3 insulation coating produced using sol–gel method. *Mater. Des.* **2016**, *109*, 390–395. [CrossRef]

33. Liu, D.; Wu, C.; Yan, M. Investigation on sol–gel Al2O3 and hybrid phosphate-alumina insulation coatings for FeSiAl soft magnetic composites. *J. Mater. Sci.* **2015**, *50*, 6559–6566. [CrossRef]

34. Lefèvre, G. In situ Fourier-transform infrared spectroscopy studies of inorganic ions adsorption on metal oxides and hydroxides. *Adv. Colloid Interface Sci.* **2004**, *107*, 109–123. [CrossRef] [PubMed]

35. Sunday, K.J.; Taheri, M.L. NiZnCu-ferrite coated iron powder for soft magnetic composite applications. *J. Magn. Magn. Mater.* **2018**, *463*, 1–6. [CrossRef]

36. Olekšáková, D.; Kollár, P.; Jakubčin, M.; Füzer, J.; Tkáč, M.; Slovenský, P.; Bureš, R.; Fáberová, M. Energy loss separation in NiFeMo compacts with smoothed powders according to Landgraf's and Bertotti's theories. *J. Mater. Sci.* **2021**, *56*, 12835–12844. [CrossRef]

37. Olekšáková, D.; Kollár, P.; Neslušan, M.; Jakubčin, M.; Füzer, J.; Bureš, R.; Fáberová, M. Impact of the Surface Irregularities of NiFeMo Compacted Powder Particles on Irreversible Magnetization Processes. *Materials* **2022**, *15*, 8937. [CrossRef]

38. Kollár, P.; Birčáková, Z.; Füzer, J.; Bureš, R.; Fáberová, M. Power loss separation in Fe-based composite materials. *J. Magn. Magn. Mater.* **2013**, *327*, 146–150. [CrossRef]

39. Talaat, A.; Suraj, M.; Byerly, K.; Wang, A.; Wang, Y.; Lee, J.; Ohodnicki, P. Review on soft magnetic metal and inorganic oxide nanocomposites for power applications. *J. Alloy. Compd.* **2021**, *870*, 159500. [CrossRef]

40. Hsiang, H.-I. Progress in materials and processes of multilayer power inductors. *J. Mater. Sci. Mater. Electron.* **2020**, *31*, 16089–16110. [CrossRef]

41. Monier-Vinard, E.; Bissuel, V.; Dia, C.T.; Daniel, O.; Laraqi, N. Investigation of Delphi Compact Thermal Model Style for Modeling Surface-Mounted Soft Magnetic Composite Inductor. In Proceedings of the 19th International Workshop on Thermal Investigations of ICs and Systems (THERMINIC), Berlin, Germany, 25–27 September 2013.